Stable passivation of cut edges in encapsulated n-type silicon solar cells using Nafion polymer

Chen, Ning; Tune, Daniel; Buchholz, Florian; Roescu, Razvan; Zeman, Miro; Isabella, Olindo; Mihailetchi, Valentin D.

Important note
To cite this publication, please use the final published version (if applicable).
Please check the document version above.

Stable passivation of cut edges in encapsulated n-type silicon solar cells using Nafion polymer

Ning Chen [a,b,*], Daniel Tune [a,**], Florian Buchholz [a], Razvan Roescu [a], Miro Zeman [b], Olindo Isabella [b], Valentin D. Mihailetchi [a]

[a] International Solar Energy Research Center (ISC) Konstanz, Rudolf-Diesel-Str. 15, Konstanz, 78467, Germany
[b] Photovoltaic Materials and Devices Group, Delft University of Technology, Mekelweg 4, Delft, 2628 CD, The Netherlands

ARTICLE INFO

ABSTRACT

In this study, the edge passivation effectiveness and long-term stability of Nafion polymer in n-type interdigitated back contact (IBC) solar cells are investigated. For new module technologies such as half-cut, triple-cut, or shingled modules, cutting of the cells introduces unpassivated edges with a high recombination rate and this limits the module power. These cut edges can be "repassivated" after cutting and in this work Nafion polymer is used to achieve this. First, different edge types, namely emitter edges (n+/n/p+) and back surface field (BSF) edges (n+/n/n+), as well as different cutting techniques such as laser cut and cleave (L&C), thermal laser separation (TLS), and mechanical cleaving are evaluated. It is found that TLS and mechanical cleaving enable good repassivation on both BSF and emitter edges. Second, industrial-size IBC solar cells are made to assess the effect of the edge repassivation on performance. On 1/4-cut M2 size IBC cells with two emitter edges, efficiency is improved by over $0.3\%_{abs}$. However, an efficiency improvement was not observed for similar cells with BSF edges, due to an insufficient passivation at the bulk edges. Last, the real-world stability of the Nafion repassivation is evaluated in industrially relevant module stacks by laminating the repassivated wafers with ethylvinylacetate (EVA) or polyolefin elastomer (POE) encapsulants and then exposing them to industry standard testing of 1000 h under damp heat conditions (85 °C, 85% relative humidity). The tests reveal that the repassivation is stable in EVA encapsulants but not in POE.

1. Introduction

The passivation of silicon solar cells has been continuously developed for many years and the combination of advanced cell structures with different passivation materials has been key to boosting the conversion efficiency. Since aluminum back surface field (Al-BSF) solar cells were introduced, the front n+emitter in p-type silicon solar cells has been well passivated with SiN_x. Likewise, on passivated emitter and rear cells (PERC), the rear side is well passivated with Al_2O_3 [1]. Passivation strategies have also been developed for metal contact areas and these are commonly used in n-type solar cells. Examples include tunnel oxide passivated contacts (TOPCon) cells, where the passivation is based on polysilicon/SiO_x structures [2], and silicon heterojunction (SHJ) solar cells based on the passivation of amorphous silicon [3]. In contrast, edge passivation is generally less effective than surface passivation. However, the edges also play a significant role in the efficiency of solar cells. For traditional Al-BSF cells, Wong et al. state that "there can be ~0.25%–0.6% absolute efficiency gain if the peripheral and edge

recombination sources are eliminated" [4]. PERC cells show better edge passivation than Al-BSF cells, with edge recombination losses up to $0.2\%_{abs}$ for a 21% efficient M0 size (156 mm × 156 mm) cell [5]. The TOPCon cell concept has an edge recombination loss of $0.5\%_{abs}$ based on the modeling of an M0 cell with a full edge recombination and without edge recombination [6]. The SHJ cells suffer edge recombination losses due to both imperfect edge passivation and the transparent conductive oxide (TCO) gap that prevents short circuits from front to back [7]. Advanced module technologies such as half-cut, triple-cut, or shingled modules can provide significant increases in module power. However, the cutting and/or cleaving processes introduce new unpassivated edges which cause additional edge recombination and reduce the efficiency potential. For high efficiency solar cells such as TOPCon and SHJ cells, edge recombination has a greater effect on absolute efficiency losses after cutting than for lower efficiency PERC cells. When the cell area becomes small with a high edge-to-area ratio, the edge recombination effects become more severe.

The traditional industrial solution for edge treatment focuses primarily on isolation of the edge [8]. Edge passivation is mainly achieved as a beneficial side effect of the surface passivation process of a solar cell and there is no cost-effective industrial solution for passivating just the cut edges of half, triple or shingled cells. In the lab, researchers have developed several small-scale solutions, including:

- Partially passivating the edges during front-end processes [9,10].
- Creating a structure to avoid cutting through the emitter region. For example, the emitter window approach or similar [11,12], or simply cutting through BSF regions for interdigitated back contact (IBC) solar cells [13].
- Using advanced cutting methods to reduce laser damage. Mechanical damage can be reduced using thermal laser separation (TLS) [14,15], and module power gains have been reported [16]. Another method is to cleave without causing any laser damage to the edge. For this, the wafers should be cut from the ingot such that the crystal orientation is parallel to the wafer edges [17].
- Passivating the edge using Al_2O_3 after laser cutting, namely "Passivated Edge Technology" [18]. Using this technique, very good passivation has been achieved on both PERC and SHJ cells [18–21].

Among the methods, the Al_2O_3 passivation method has great potential to become a standard process for industry. However, there are still bottlenecks to overcome. For example, the Al_2O_3 is usually deposited under vacuum and in heated conditions, and post annealing or thermal treatment is needed to activate the passivation.

As an alternative, it is possible to use the very strong field effect passivation provided by certain Lewis acid organic polymer thin films, especially the so-called superacids. After the first reports of silicon surface passivation from Biro and Warta in 1998–2002 [22,23], this technique has been attracting significant renewed interest in recent years, starting with the 2016 reports of Bullock et al. [24] and Hossain et al. [25] and continuing through a growing number of other works [26–31]. Compared to other methods of silicon surface passivation, these organic polymer films have the advantage that they can be deposited at room temperature using non-vacuum processes such as spin-, dip-, spray- or slot-die coating. Of the various superacids studied, Nafion (sulfonated tetrafluoroethylene) is particularly promising for industrial application due to its relatively low reactivity and thus stability potential. Recently, we extended the application of Nafion passivation to the edges of laser-cut silicon solar cells and demonstrated the critical importance of the morphology of the edge surface, whether laser damaged or cleanly cleaved, in determining the extend of edge passivation achievable through this technique [32,33]. Similarly, Li et al. used Nafion edge passivation on a 9 cm^2 SHJ cell, showing a V_{oc} improvement of 8 mV, and an improvement of 1–2%$_{abs}$ in efficiency [34], while Chen et al. showed that an alkaline etching and cleaning procedure can improve the edge passivation by removing laser damage [35].

In this work, we further extend the Nafion edge passivation concept through a systematic study on industrial size n-type silicon solar cells. The edge passivation is applied on the newly cut or cleaved edges to recover partly the cut losses, which is also referred to as edge repassivation hereafter. Different types of industrially relevant cut edges were evaluated, including emitter edges (n+/n/p+) and BSF edges (n+/n/n+), as well as different cutting techniques. The edge repassivation was tested on n-type IBC solar cells and electrical parameters were compared before and after repassivation. Importantly for commercial application, we show for the first time that the Nafion passivation can withstand the accelerated damp-heat testing regime of the IEC 61215 industrial qualification standard for photovoltaic modules when the modules are manufactured using a standard industrial bill of materials.
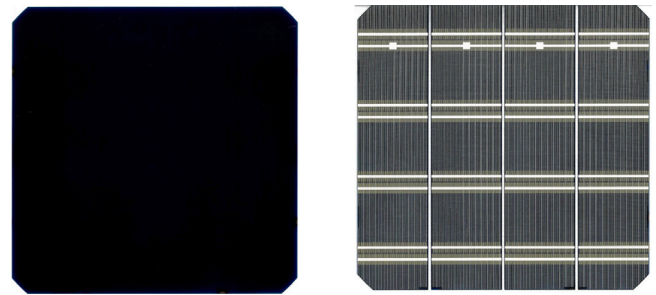

Fig. 1. Images of a solar cell fabricated for edge repassivation evaluation. The left image is the front side of a cell. The right image is the rear side of a cell, and the cell was cut into 1/4 sizes through the gaps.

Table 1
Solar cells' IV changes (Δ) after repassivation, with and without HF clean. Cells are TLS emitter cut with 1-edge.

Group	Cell number	ΔV_{oc} (mV)	ΔJ_{sc} (mA/cm^2)	ΔFF (%)	$\Delta\eta$ (%)
HF clean	3	-0.10 ± 0.13	0.08 ± 0.00	0.31 ± 0.07	0.13 ± 0.03
non-HF clean	3	0.26 ± 0.07	0.19 ± 0.02	0.31 ± 0.05	0.15 ± 0.04

2. Experimental

2.1. Lifetime and solar cell samples

M2 (156.75 mm × 156.75 mm) n-type Czochralski (CZ) (100) oriented wafers, with a thickness of 175 μm and a base resistivity of 4 ±1 Ω cm were used as lifetime test structures as well as solar cell samples. All wafers were saw damage etched in a KOH solution and cleaned in a piranha solution. The emitter edge samples were doped using BBr_3 and $POCl_3$ diffusion, respectively. The BSF edges samples were first textured in a KOH bath with a texture additive, and then double-sided diffused with $POCl_3$. Solar cells were fabricated using our best-known method (BKM) described previously [36,37]. One of the features is that the passivation layer was in-situ grown SiO_2 and then capped with SiN_x [38].

The IBC cells were designed to be cut into 1/4 sizes through either the emitter or BSF regions [13], and the images are shown in Fig. 1. The lifetime samples were cut into 4 mm × 4 mm. Different methods were used to cut the edges, including (1) TLS cut, using an industrial tool (3D-Micromac); (2) Laser cut and cleave (L&C) using a nanosecond laser with a laser damage depth around 80 μm (F20, InnoLas); (3) Cleaving was done manually. After scribing the wafer edge with a diamond pen, the wafer edge was manually cleaved to a 45° angle.

2.2. Edge repassivation using Nafion

Nafion perfluorinated resin solution, 5 wt% in mixture of lower aliphatic alcohols and water, contains 15%–20% water, from Sigma-Aldrich was used in the study. To remove native oxide from the wafer edges, the wafer edges were dipped into 5vol.% HF for 10 s followed by a DI water rinse and N_2 blow drying.

Passivation was achieved by dipping the cell edges in Nafion solution for 10 s, followed by N_2 blow drying. In the case of solar cell repassivation, two groups of solar cells were also tested with and without HF cleaning before Nafion, to check whether the HF cleaning can be skipped (to avoid HF corrosion to solar cells). The edge of the cell was dipped into Nafion solution and then dried with N_2. The process flow of edge repassivation on solar cells is shown in Fig. 2.
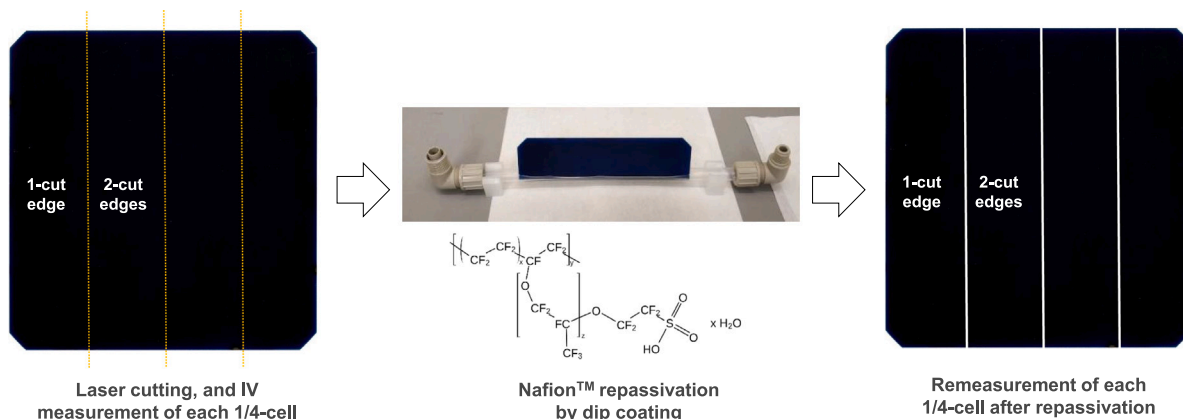
Fig. 2. Process flow of edge repassivation on solar cells. M2 size IBC solar cells were cut into 1/4 sizes; then repassivated by Nafion using dip coating.
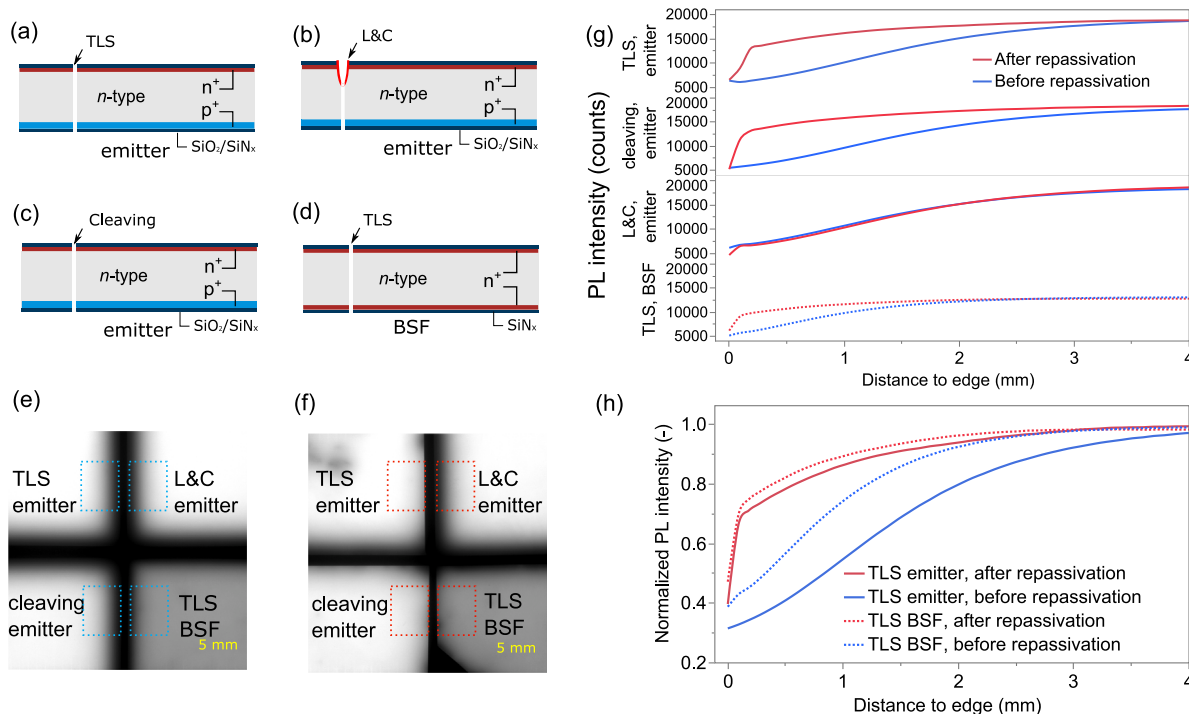

Fig. 3. Samples for edge repassivation evaluation and results. (a), (b), (c), and (d) are n-type silicon wafer samples with different types of edges; (e) shows PL images of the (a–d) samples before Nafion repassivation while (f) shows PL images of the samples after Nafion repassivation; (g) shows PL intensity profiles of different types of edges before and after repassivation, measured from the square areas marked in (e) and (f); (h) shows normalized PL intensity profiles (measured PL intensity divided by maximum of PL intensity of each curve) of TLS edges before and after repassivation.

2.3. PL and IV characterizations

Photoluminescence (PL) and IV were measured for the samples to evaluate the edge repassivation. The PL was measured using a custom-built PL system (ISC Konstanz), integrated with a macro lens described in a previous publication [33]. A Class AAA xenon flasher (Halm Elektronik) was used for IV characterization under standard test conditions. A measurement chuck, based on printed circuit board technology, was specifically designed for back contact cells.

2.4. Encapsulated samples and damp heat tests

The wafer samples were laminated in a solar module laminator (Phototrade - P. Energy). Module structure comprises 2 mm thick glass and transparent backsheet (Dunmore DS450). In the case of EVA, the lamination temperature is 145 °C, and the lamination time is 10 min; the lamination temperature for POE is 150 °C, and the lamination time is 13 min. The damp heat test was conducted in a climate chamber (Vötsch) at 85 °C, 85% relative humidity for 1000 h in accordance with IEC 61215. The PL was measured at various intervals during the test, including before lamination, after lamination, at DH 0 h, 25 h, 100 h, 260 h, 500 h, 785 h, and 1000 h.

3. Results and discussion

3.1. Nafion passivation of the different edges

PL is a useful tool for qualitative lifetime analysis of wafers as well as the passivation of their edges [39,40]. A high-resolution PL imaging technique was used in this study for the evaluation of edge

Table 2
Solar cells' IV changes (Δ) after repassivation.

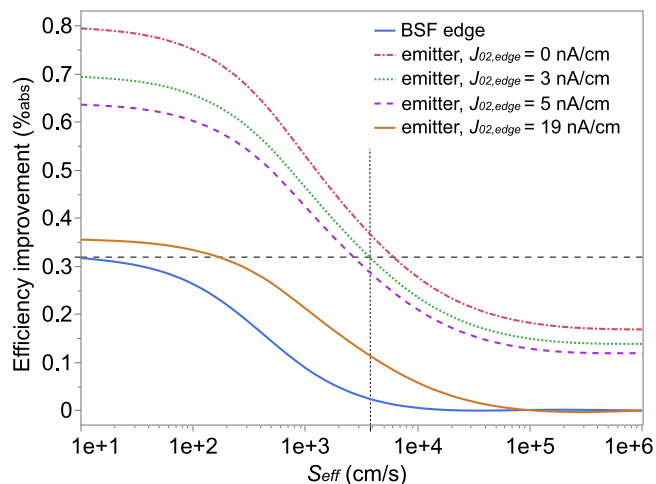| Group	Cell number	ΔV_{oc} (mV)	ΔJ_{sc} (mA/cm^2)	ΔFF (%)	$\Delta\eta$ (%)
L&C, BSF 1-edge	3	0.02 ± 0.22	-0.02 ± 0.00	-0.03 ± 0.02	-0.02 ± 0.00
L&C, emitter 1-edge	3	-0.05 ± 0.04	-0.01 ± 0.00	-0.05 ± 0.02	-0.01 ± 0.02
TLS, emitter 1-edge	6	**0.10 ± 0.19**	**0.08 ± 0.01**	**0.31 ± 0.08**	**0.14 ± 0.03**
TLS, emitter 2-edge	5	**0.76 ± 0.11**	**0.17 ± 0.01**	**0.68 ± 0.10**	**0.32 ± 0.04**
TLS, BSF 1-edge	6	-0.16 ± 0.14	0.01 ± 0.01	-0.03 ± 0.02	0.00 ± 0.01
TLS, BSF 2-edge	5	0.18 ± 0.25	0.00 ± 0.02	-0.01 ± 0.05	0.01 ± 0.03
Reference (no repassivation)	5	-0.03 ± 0.24	0.00 ± 0.04	-0.01 ± 0.09	0.00 ± 0.02

Fig. 4. Quokka3 simulation results of potential efficiency improved with different edge recombination parameters. The simulation was done for a M2 1/4-cell with two recombining edges, either BSF or emitter edges. Efficiency improvement was simulated compared with cells with very high edge recombination ($J_{02,\ edge} = 19$ nA/cm and recombination of qn bulk $S_{eff} = 10^6$ cm/s. The horizontal dashed line represents the 0.32%$_{abs}$ efficiency improvement measured on emitter cells, and the vertical dotted line corresponds to the S_{eff} value at which $J_{02,\ edge} = 3$ nA/cm.

passivation [32] and both lifetime samples and solar cells can be quickly evaluated using this technique. Lifetime samples were prepared to represent different types of edges and cutting methods of n-type cells. Based on the cell structure, there can be two types of wafer edges, emitter edges (n+/n/p+) and BSF edges (n+/n/n+). Depending on the application, emitter edges might represent (1) all front and rear contact cells edges when the cut is always through emitter regions or (2) for IBC cells, when the cut is through emitter regions. The BSF edges represent a special case for IBC cells, when the cut is through BSF regions. Additionally, different cutting methods were also evaluated, including TLS, L&C [41], and mechanical cleaving. Four types of edges were included in the test as shown in Fig. 3:

- (a) Emitter edge (n+/n/p+) with TLS cut;
- (b) Emitter edge (n+/n/p+) with L&C on the n+side;
- (c) Emitter edge (n+/n/p+) with no laser damage, only cleaving through the emitter regions;
- (d) BSF edge (n+/n/n+) with TLS cut.

Qualitative differences in edge repassivation of the four types of samples can be clearly observed in the PL images shown in Fig. 3. Prior to repassivation (Fig. 3(e)), all edges appear blurry and indistinct from the black background. However, after repassivation (Fig. 3(f)) the TLS-cut and the mechanically cleaved edges have become much sharper and are clearly distinguishable from the black background, indicating an improvement in edge passivation.

To better quantify the effect of edge repassivation, the PL intensity of different samples was plotted along a line from the wafer edge (0 mm) towards the center of the wafer up to a distance of 4 mm and

the resulting PL intensity profiles are shown in Fig. 3(g) for each type of cutting process. The blue curves were taken from the PL images before repassivation whereas the red curves from the images after Nafion repassivation. For all samples, the PL signal increases gradually from the edge towards the center of the wafer and saturates at a level limited by bulk and surface passivation (a typical distance of several times the minority carrier diffusion length).

In the case of emitter samples (the upper three plots of Fig. 3(g), and shown schematically in Fig. 3(a–c)), the profiles before repassivation are similar. After repassivation, TLS and mechanical cleaving show similar repassivation effectiveness as indicated by identical PL profiles. There was no repassivation on the L&C sample due to severe laser damage to the edge. For repassivation, a smooth cut edge (from either TLS or 45° cleaving) is essential [42]. In the TLS BSF samples (with TLS cut through the n+/n/n+edge), the initial passivation quality is poor due to the passivation of BSF samples is not as good as that of the emitter samples. A better comparison of repassivation between BSF and emitter samples can be achieved by comparing normalized PL profile curves as shown in Fig. 3(h). By normalizing the PL profile curves, the initial passivation difference between the two samples can be excluded. From 3(h) we observed that the TLS BSF cut edge shows better repassivation than TLS emitter cut edge before repassivation process. Whereas after repassivation the two profiles are similar to each other. A quantitative modeling of edge recombination using Quokka3 tool was previously presented by Fell [6]. This simulation model accounts for the recombination at the edge from the space-charge-region (SCR) of the emitter and the quasi-neutral (qn) bulk of the Si base. Thus, for BSF cut edges, only the qn recombination losses are dominant. For the emitter cut edges, the recombination losses are caused from both SCR and qn regions. Before repassivation, the difference between them was the SCR recombination. Following repassivation, the PL profiles of both edges become similar, indicating a significant reduction in SCR recombination. The repassivation quality of both edges after repassivation is constrained by the qn bulk edge.

3.2. Repassivation on solar cells

To evaluate the Nafion repassivation at the cell level, n-type IBC solar cells were prepared. M2 size IBC cells were prepared and cut into 1/4 sizes using TLS and L&C. Nafion repassivation was performed using dip coating and the IV characteristic were measured before and after repassivation.

First, a test was conducted to determine whether the HF cleaning step could be skipped. The results are summarized in Table 1. As can be seen in Table 1, a similar efficiency gain can be achieved without the use of HF cleaning. The presence of native SiO_x on the edge has the potential to influence the repassivation quality of Nafion and is usually removed by HF etching. However, Table 1 shows that no improvement in repassivation quality was observed after additional HF etching before Nafion treatment. For a cost-effective industrial process, this HF etching post metallization should anyway be avoided. In the following experiment, all cells were treated without HF cleaning.

Different groups of samples were evaluated including different cutting methods (L&C and TLS), different edge types (emitter and BSF edges), as well as different cut-edge numbers (1-edge and 2-edge),
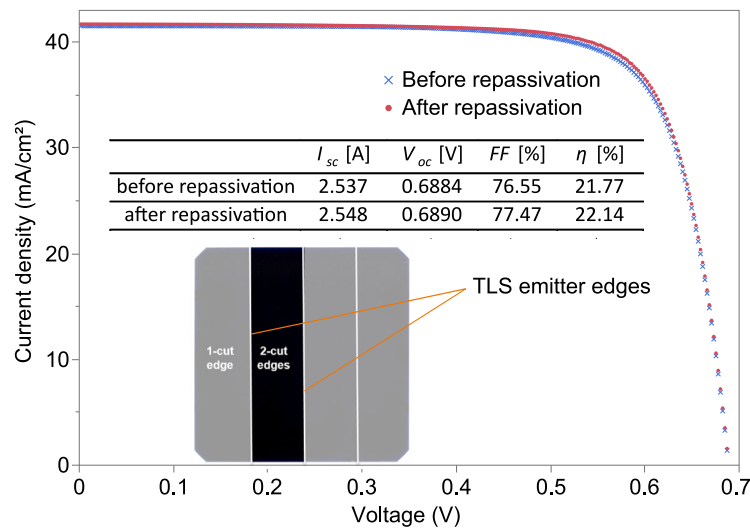
Fig. 5. IV curves measured on a 1/4 M2 cell before (blue cross) and after repassivation (red dots), the cell was with 2-edge cut through emitter by TLS. The IV parameters and the cell images are also indicated.
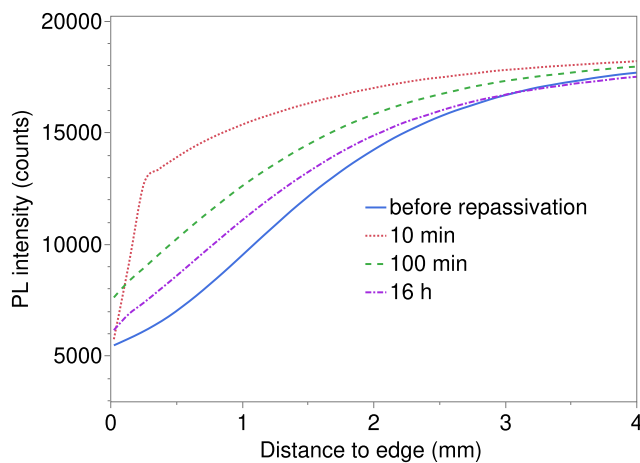

Fig. 6. PL results of edge repassivation over time, when the edge was exposed in the air.

and reference samples (L&C BSF cut cells with 2-edge) without repassivation were also measured to confirm the repeatability. Table 2 summarizes the IV results in detail. No repassivation was observed on either BSF or emitter edges of L&C cut samples. On TLS emitter cut samples, a clear improvement in efficiency was observed. In 1-edge cells, efficiency was improved by $0.14\%_{abs}$; and in 2-edge cells, efficiency was improved by $0.32\%_{abs}$. However, on BSF cut samples, no repassivation was observed. Factors contributing to this include:

- The edge recombination on BSF samples is relatively small. This is demonstrated by the Quokka3 simulation results in Table 3, which show the change in the IV parameters of a 1/4-cell with and without edge recombination. These simulation results were taken from [13] and were confirmed by the experimental data. As can be seen from Table 3, when cutting through the BSF regions, the efficiency losses are only around one-third compared with cutting through emitter regions. Therefore the potential efficiency gain from repassivation is relatively small for BSF cut region. For emitter samples, there was approximately 30 to $40\%_{rel}$ of initial efficiency loss was recovered by Nafion repassivation.
- Quokka3 simulation was performed to evaluate how SCR (defined by $J_{02, edge}$) and qn bulk edge (defined by S_{eff}) recombination

parameters influence the cell efficiency. The results are shown in Fig. 4. The simulation results agree with the experimental observed 2-edge repassivation improvement for TLS cut emitter and BSF cells in Table 2 if one assume a $J_{02, edge} \leq 3$ nA/cm and a S_{eff} in a range of 4000–8000 cm/s. By comparing the $J_{02, edge}$ and S_{eff} values required to fit the experimental cut cells before and after repassivation, one can see that the largest effect of Nafion repassivation consist in significant reduction of edge SCR recombination ($J_{02, edge}$). The additional reduction in S_{eff} from $S_{eff} = 10^6$ cm/s to $S_{eff} = 4000$ cm/s only seems to be beneficial for emitter cut. For BSF cut cells a S_{eff} below ~ 1000 cm/s would be needed to observe a repassivation effect.
- The final significant factor to consider is the uniformity of repassivation along the cut edge. From PL measurements, it was observed that the repassivation uniformity on solar cells is lower than that on lifetime samples. The PL profiles for the lifetime samples in Fig. 3 are taken locally in a part of the cut edge with fewer defects in order to assess the maximum repassivation capability whereas the solar cell IV measurements take into account the effect of repassivation over the entire length of the cut edge. This non uniformity in the edge repassivation effect may explain the apparent discrepancy between the results on lifetime samples and the magnitude of the efficiency improvements upon Nafion treatment of the BSF and emitter cut cells. Therefore, it is conceivable that by improving the uniformity of the repassivation by Nafion treatment of the cut edge, a higher improvement in cell efficiency would be possible. The potential for such improvements is shown in Fig. 4 if one assume further reduction in $J_{02, edge}$ and especially in S_{eff} values.

Nevertheless, an average of $0.32\%_{abs}$ efficiency gain from Nafion edge repassivation is still significant improvement. One of the best cells with repassivation on two edges can be observed in the IV curves shown in Fig. 5. It is evident from the IV curve and IV parameters that the improvement was predominantly due to increased FF, with only slight improvements in J_{sc} and V_{oc}.

3.3. Damp heat test results

In air, the Nafion repassivation is not stable and the edge repassivation effect on the solar cell level rapidly wears off. This can be readily observed in Fig. 6, where the initially excellent repassivation of an unencapsulated TLS emitter cut sample degrades over several hours
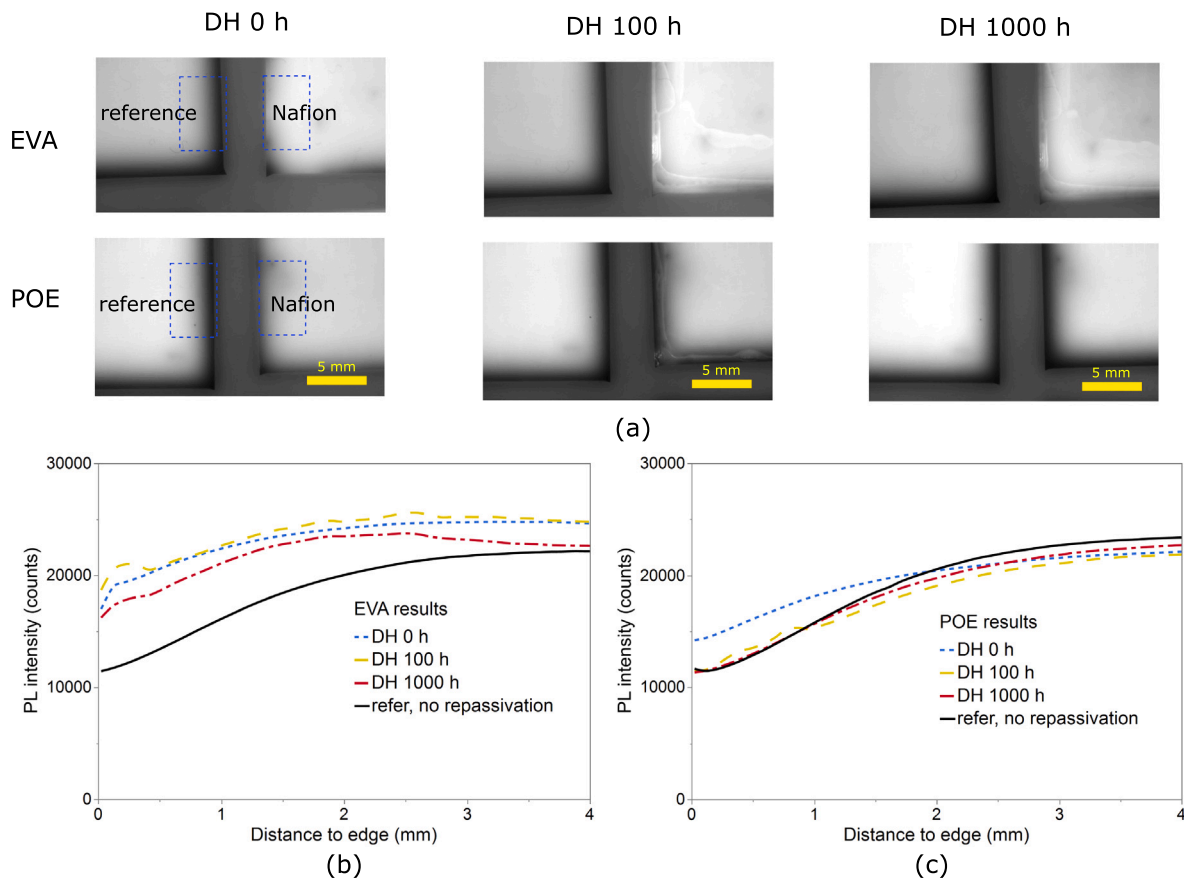
Fig. 7. PL results of samples encapsulated with either EVA or POE and tested before and after exposure to damp heat (DH) conditions. The results of the PL measurements were taken before DH (DH0), after 100 h of damp heat exposure (DH100), and after 1000 h (DH1000), measured from the square areas marked. The normalized PL intensity profiles of Nafion passivated edges in EVA and POE are shown in (b) and (c), respectively.

of air exposure. The degradation can be observed from the gradient changes (from sharp to flat) of PL profiles measured at different time intervals.

An adhesive foil has been used in previous studies to protect the Nafion passivated samples from degrading [23]. However, this solution is not relevant for industrial production where several standard encapsulating materials are instead used to protect the solar cells. In this work, we studied whether or not such standard industrial encapsulation materials can preserve the passivation, as well as whether the Nafion passivation can withstand the heating and mechanical pressures introduced during the module assembly process.

After assembling modules with standard industrial processes and materials, the stability of the edge repassivation was evaluated by damp heat (DH) testing according to the IEC 61215 standard. For the evaluation of edge repassivation stability, lifetime samples and high-resolution PL were again used. TLS cut samples were used since these showed encouraging results in the previous experiment and the tools are already commercially available. Samples were encapsulated with ethylene vinyl acetate (EVA) or polyolefin elastomers (POE) in a glass/backsheet structure.

PL images taken immediately after encapsulation and after 100 h of damp heat exposure (DH100) and 1000 h of exposure (DH1000) are shown in Fig. 7(a). Combined with the PL intensity plots shown in Figs. 7(b) and 7(c), these show the extent of the repassivation effect of Nafion following the lamination process with both EVA and POE, as well as clearly demonstrating that the repassivation can survive the lamination process. However, the level of repassivation after lamination reduced in the POE case (starting point at $x = 0$ mm), relative to that of the EVA (starting point at $x = 0$ mm). In addition, significant differences are observed between the rates of degradation of the

Table 3
Quokka3 simulation results from [13], solar cells' IV changes (Δ) before and cutting.

Group	ΔV_{oc} (mV)	ΔJ_{sc} (mA/cm^2)	ΔFF (%)	$\Delta \eta$ (%)
emitter 1-edge	−2.04	−0.09	−1.15	−0.45
emitter 2-edge	−3.97	−0.19	−2.20	−0.85
BSF 1-edge	−0.84	−0.17	−0.16	−0.17
BSF 2-edge	−1.68	−0.33	−0.32	−0.33

repassivation using EVA and POE, with the repassivation almost fully degraded after only 100 h in POE but with the repassivation remaining relatively stable even after 1000 h in EVA. POE is usually preferred over EVA for encapsulation, especially for n-type solar cell because of its better resistance against potential-induced degradation (PID) and superior moisture barrier performance. However, this work clearly demonstrates that EVA performs better in regards to maintaining the repassivation effect of the Nafion polymer.

4. Conclusion

In this study, edge repassivation of cut n-type silicon IBC solar cells using Nafion polymer was investigated. It was shown that Nafion can be used to passivate the cut edges of both n+/n/n+and n+/n/p+structures, but that the repassivation is more effective on n+/n/p+structures (a solar cell) than on n+/n/n+structures (a symmetric BSF sample). Furthermore, the effectiveness of the repassivation depends strongly on the cutting method used, with edges that have less laser damage after cutting (such as TLS) or mechanically cleaved edges being more susceptible to repassivation. An efficiency improvement of

over 0.3%$_{abs}$ was measured on 1/4-cut M2-size IBC solar cells with TLS cut emitter (n+/n/p+) edges, but there was no edge passivation observed on cut edges of symmetric n+/n/n+structures or on solar cells with L&C cuts which is limited by passivation on bulk edge region. Importantly for industrial application of this material, encapsulation using EVA and POE were demonstrated to provide protection of the passivation through the solar module lamination process. However, only the EVA encapsulation provided protection against degradation of the passivation over time, with the edge passivation remaining stable even in harsh damp heat conditions (85 °C, 85% relative humidity) for 1000 h as per the IEC 61215 standard. In contrast, POE failed to provide such protection, with almost complete degradation of the encapsulant with only 100 h of damp heat exposure.

In summary, this work has shown that Nafion polymer can be used to repassivate the edges of cut n-type solar cells, but that the degree of repassivation provided depends heavily on the method used to cut the cells. Furthermore, this work has also shown for the first time that the repassivation provided by this material can be stable under harsh accelerated aging conditions when encapsulated with industrial standard EVA polymer. The repassivation can be achieved with a simple solution process at room temperature and without the use of vacuum, and this process could be simply integrated into the inline wet chemistry tools of industrial module manufacturing lines. Further research is necessary to improve the repassivation of n-type bulk regions and achieve uniform passivation on cell edges. Additionally, it is important to investigate the observed degradation in POE samples. Nevertheless, the results of this work firmly establish the viability of Nafion polymer, or analogues thereof, for edge passivation of industrial solar cells.

CRediT authorship contribution statement

Ning Chen: Writing – original draft, Methodology, Investigation. **Daniel Tune:** Writing – original draft, Methodology, Conceptualization. **Florian Buchholz:** Writing – review & editing, Project administration, Conceptualization. **Razvan Roescu:** Resources, Investigation. **Miro Zeman:** Writing – review & editing, Supervision. **Olindo Isabella:** Writing – review & editing, Supervision. **Valentin D. Mihailetchi:** Writing – original draft, Supervision, Project administration.

Declaration of competing interest

The authors declare that they have no known competing financial interests or personal relationships that could have appeared to influence the work reported in this paper.

Data availability

Data will be made available on request.

Acknowledgments

References

[1] B. Hoex, J. Schmidt, P. Pohl, M. Van de Sanden, W. Kessels, Silicon surface passivation by atomic layer deposited Al$_2$O$_3$, J. Appl. Phys. 104 (4) (2008) 044903.

[2] F. Feldmann, M. Bivour, C. Reichel, M. Hermle, S.W. Glunz, Passivated rear contacts for high-efficiency n-type Si solar cells providing high interface passivation quality and excellent transport characteristics, Sol. Energy Mater. Sol. Cells 120 (2014) 270–274.

[3] S. De Wolf, A. Descoeudres, Z.C. Holman, C. Ballif, High-efficiency silicon heterojunction solar cells: A review, Green 2 (1) (2012) 7–24.

[4] J. Wong, R. Sridharan, V. Shanmugam, Quantifying edge and peripheral recombination losses in industrial silicon solar cells, IEEE Trans. Electron Devices 62 (11) (2015) 3750–3755.

[5] A. Fell, P.P. Altermatt, Detailed 3D full-cell modeling in Quokka3: Quantifying edge and solder-pad losses in an industrial PERC cell, in: AIP Conference Proceedings, Vol. 1999, AIP Publishing LLC, 2018, 020007.

[6] A. Fell, J. Schön, M. Müller, N. Wöhrle, M.C. Schubert, S.W. Glunz, Modeling edge recombination in silicon solar cells, IEEE J. Photovolt. 8 (2) (2018) 428–434.

[7] V. Giglia, R. Varache, J. Veirman, E. Fourmond, Influence of cell edges on the performance of silicon heterojunction solar cells, Sol. Energy Mater. Sol. Cells 238 (2022) 111605.

[8] T. Dannenberg, J. Vollmer, M. Passig, C. Scheiwe, D. Brunner, A. Pediaditakis, U. Jäger, I. Wang, W. Xie, S. Xu, et al., Past, present, and future outlook for edge isolation processes in highly efficient silicon solar cell manufacturing, Solar RRL (2022) 2200594.

[9] C. Chan, M. Abbott, B. Hallam, M. Juhl, D. Lin, Z. Li, Y. Li, J. Rodriguez, S. Wenham, Edge isolation of solar cells using laser doping, Sol. Energy Mater. Sol. Cells 132 (2015) 535–543.

[10] S. Schäfer, F. Haase, C. Hollemann, J. Hensen, J. Krügener, R. Brendel, R. Peibst, 26%-Efficient and 2 cm narrow interdigitated back contact silicon solar cells with passivated slits on two edges, Sol. Energy Mater. Sol. Cells 200 (2019) 110021.

[11] D. König, G. Ebest, New contact frame design for minimizing losses due to edge recombination and grid-induced shading, Sol. Energy Mater. Sol. Cells 75 (3–4) (2003) 381–386.

[12] K. Rühle, M.K. Juhl, M.D. Abbott, L.M. Reindl, M. Kasemann, Impact of edge recombination in small-area solar cells with emitter windows, IEEE J. Photovolt. 5 (4) (2015) 1067–1073.

[13] N. Chen, F. Buchholz, D.D. Tune, O. Isabella, V.D. Mihailetchi, Mitigating cut losses in interdigitated back contact solar cells, IEEE J. Photovolt. 12 (6) (2022) 1386–1392.

[14] F. Kaule, M. Pander, M. Turek, M. Grimm, E. Hofmueller, S. Schoenfelder, Mechanical damage of half-cell cutting technologies in solar cells and module laminates, in: AIP Conference Proceedings, Vol. 1999, AIP Publishing LLC, 2018, 020013.

[15] H. Han, X. Jia, C. Ma, Y. Wu, A novel laser scribing method combined with the thermal stress cleaving for the crystalline silicon solar cell separation in mass production, Sol. Energy Mater. Sol. Cells 240 (2022) 111714.

[16] C. Zhang, H. Shen, H. Liu, W. Zhang, J. Chen, H. Li, Influence of laser condition on the electrical and mechanical performance of bifacial half-cutting PERC solar cell and module, Int. J. Energy Res. 46 (11) (2022) 15290–15299.

[17] J. Lelièvre, S. Harrison, M. Albaric, L. Carton, B. Portaluppi, V. Barth, Alternative CZ ingot squaring and half-cell cutting methodology for low-temperature PV cell and module technologies, in: Proc. 37th Eur. Photovolt. Sol. Energy Conf, 2020, pp. 487–489.

[18] P. Baliozian, M. Al-Akash, E. Lohmüller, A. Richter, T. Fellmeth, A. Münzer, N. Wöhrle, P. Saint-Cast, H. Stolzenburg, A. Spribille, et al., Postmetallization "passivated edge technology" for separated silicon solar cells, IEEE J. Photovolt. 10 (2) (2020) 390–397.

[19] A. Münzer, P. Baliozian, A. Steinmetz, T. Geipel, S. Pingel, A. Richter, S. Roder, E. Lohmüller, A. Spribille, R. Preu, Post-separation processing for silicon heterojunction half solar cells with passivated edges, IEEE J. Photovolt. 11 (6) (2021) 1343–1349.

[20] S. Harrison, B. Portaluppi, P. Bertrand, V. Giglia, B. Martel, A. Sekkat, D. Munoz-Rojas, Low temperature post-process repassivation for heterojunction cut-cells, in: 38th European Photovoltaic Solar Energy Conference and Exhibition, 2021, pp. 167–171.

[21] B. Martel, M. Albaric, S. Harrison, F. Dhainaut, T. Desrues, Addressing separation and edge passivation challenges for high efficiency shingle heterojunction solar cells, Sol. Energy Mater. Sol. Cells 250 (2023) 112095.

[22] D. Biro, W. Warta, German patent, 1998, Google Patents, DE198 57 064.3-33.

[23] D. Biro, W. Warta, Low temperature passivation of silicon surfaces by polymer films, Sol. Energy Mater. Sol. Cells 71 (3) (2002) 369–374.

[24] J. Bullock, D. Kiriya, N. Grant, A. Azcatl, M. Hettick, T. Kho, P. Phang, H.C. Sio, D. Yan, D. Macdonald, et al., Superacid passivation of crystalline silicon surfaces, ACS Appl. Mater. Interfaces 8 (36) (2016) 24205–24211.

[25] J. Hossain, Q. Liu, T. Miura, K. Kasahara, D. Harada, R. Ishikawa, K. Ueno, H. Shirai, Nafion-modified PEDOT: PSS as a transparent hole-transporting layer for high-performance crystalline-Si/organic heterojunction solar cells with improved light soaking stability, ACS Appl. Mater. Interfaces 8 (46) (2016) 31926–31934.

[26] J. Chen, K. Ge, C. Zhang, J. Guo, L. Yang, D. Song, F. Li, Z. Xu, Y. Xu, Y. Mai, Vacuum-free, room-temperature organic passivation of silicon: Toward very low recombination of micro-/nanotextured surface structures, ACS Appl. Mater. Interfaces 10 (51) (2018) 44890–44896.

[27] I. Jeon, C. Delacou, H. Okada, G.E. Morse, T.-H. Han, Y. Sato, A. Anisimov, K. Suenaga, E.I. Kauppinen, S. Maruyama, et al., Polymeric acid-doped transparent carbon nanotube electrodes for organic solar cells with the longest doping durability, J. Mater. Chem. A 6 (30) (2018) 14553–14559.

[28] W. Ji, Y. Zhao, H.M. Fahad, J. Bullock, T. Allen, D.-H. Lien, S. De Wolf, A. Javey, Dip coating passivation of crystalline silicon by Lewis acids, ACS Nano 13 (3) (2019) 3723–3729.

[29] D.D. Tune, N. Mallik, H. Fornasier, B.S. Flavel, Breakthrough carbon nanotube–silicon heterojunction solar cells, Adv. Energy Mater. 10 (1) (2020) 1903261.

[30] J. Chen, D.D. Tune, K. Ge, H. Li, B.S. Flavel, Front and back-junction carbon nanotube-silicon solar cells with an industrial architecture, Adv. Funct. Mater. 30 (17) (2020) 2000484.

[31] J. Chen, L. Wan, H. Li, J. Yan, J. Ma, B. Sun, F. Li, B.S. Flavel, A polymer/carbon-nanotube ink as a boron-dopant/inorganic-passivation free carrier selective contact for silicon solar cells with over 21% efficiency, Adv. Funct. Mater. 30 (38) (2020) 2004476.

[32] D.D. Tune, F. Buchholz, I. Ullman, A. Halm, Measuring and mitigating edge recombination in modules employing cut cells, in: Proc. 37th Eur. Photovolt. Sol. Energy Conf, 2020, pp. 322–328.

[33] N. Chen, D. Tune, F. Buchholz, A. Halm, V. Mihailetchi, Impact of cut edge re-combination in high efficiency solar cells–Measurement and mitigation strategies, in: Proc. 38th Eur. Photovolt. Sol. Energy Conf, 2021, pp. 253–256.

[34] W. Li, X. Wang, J. Guo, X. Zhang, B. Chen, J. Chen, Q. Gao, X. Yang, F. Li, J. Wang, et al., Compensating cutting losses by passivation solution for industry upgradation of TOPCon and SHJ solar cells, in: Advanced Energy and Sustainability Research, Wiley Online Library, 2022, 2200154.

[35] K. Chen, S. Agarwal, A.R. Meyer, H. Guthrey, W. Nemeth, S. Theingi, M. Page, D.L. Young, P. Stradins, Nafion Passivation of c-Si Surface and Edge for Electron Paramagnetic Resonance, Technical Report, National Renewable Energy Lab.(NREL), Golden, CO (United States), 2022.

[36] R. Kopecek, J. Libal, J. Lossen, V.D. Mihailetchi, H. Chu, C. Peter, F. Buchholz, E. Wefringhaus, A. Halm, J. Ma, L. Jianda, G. Yonggang, Q. Xiaoyong, W. Xiang, D. Peng, ZEBRA technology: low cost bifacial IBC solar cells in mass production with efficiency exceeding 23.5%, in: 2020 47th IEEE Photovoltaic Specialists Conference, PVSC, IEEE, 2020, pp. 1008–1012.

[37] R. Kopecek, F. Buchholz, V.D. Mihailetchi, J. Libal, J. Lossen, N. Chen, H. Chu, C. Peter, T. Timofte, A. Halm, et al., Interdigitated back contact technology as final evolution for industrial crystalline single-junction silicon solar cell, in: Solar, Vol. 3, MDPI, 2022, pp. 1–14.

[38] V.D. Mihailetchi, H. Chu, J. Lossen, R. Kopecek, Surface passivation of boron-diffused junctions by a borosilicate glass and in situ grown silicon dioxide interface layer, IEEE J. Photovolt. 8 (2) (2018) 435–440.

[39] T. Trupke, R. Bardos, M. Schubert, W. Warta, Photoluminescence imaging of silicon wafers, Appl. Phys. Lett. 89 (4) (2006) 044107.

[40] K.C. Fong, M. Padilla, A. Fell, E. Franklin, K.R. McIntosh, T.C. Kho, A.W. Blakers, Y. Nebel-Jacobsen, S.R. Surve, Perimeter recombination characterization by luminescence imaging, IEEE J. Photovolt. 6 (1) (2015) 244–251.

[41] M. Oswald, M. Turek, J. Schneider, S. Schoenfelder, Evaluation of silicon solar cell separation techniques for advanced module concepts, in: Proc. 28th Eur. Photovolt. Sol. Energy Conf, 2013, pp. 1807–1812.

[42] L. Tous, J. Govaert, S. Harrison, C. Carrière, V. Barth, V. Giglia, F. Buchholz, N. Chen, A. Halm, A. Faes, et al., Overview of key results achieved in H2020 HighLite project helping to raise the EU PV industries' competitiveness, Prog. Photovolt., Res. Appl. (2023).